



Cite this: *Phys. Chem. Chem. Phys.*,
2016, **18**, 26595

Mechanistic insights into lithium ion battery electrolyte degradation – a quantitative NMR study†

S. Wiemers-Meyer,^a M. Winter^{ab} and S. Nowak^{*a}

The changes in electrolyte composition on the molecular level and the reaction mechanisms of electrolyte degradation upon thermal aging are monitored by quantitative NMR spectroscopy, revealing similar rates of degradation for pristine and already aged electrolytes. The data analysis is not in favor of an autocatalytic reaction mechanism based on OPF_3 but rather indicates that the degradation of LiPF_6 in carbonate based solvents proceeds *via* a complex sequence of “linear” reactions rather than a cyclic reaction pattern which is determined by the amount of water present in the samples. All investigated electrolytes are reasonably stable at temperatures of up to 60 °C in the presence of minor amounts or absence of water hence indicating that chemical instability of electrolyte components against water is decisive for degradation and an increase in temperature (“thermal aging”) just accelerates the degradation impact of water.

Received 29th July 2016,
Accepted 7th September 2016

DOI: 10.1039/c6cp05276b

www.rsc.org/pccp

1 Introduction

Currently, much effort is devoted to investigate the relation between chemical and physical properties and electrochemical performance of lithium ion battery materials.^{1–6} Early studies considering the electrolyte and its aging processes revealed that water and other protic impurities have a detrimental effect on the electrolyte stability at higher temperatures,^{7,8} while later the identification of degradation products (mainly from carbonate and PF_6^-) and kinetic studies came into focus thereby providing tentative reaction mechanisms^{9–14} in addition to a detailed report on degradation mechanisms of carbonate electrolyte solvents.¹⁵ Also, the applicability of various analytical methods to reliably monitor electrolyte aging processes including gas chromatography (GC),^{16–23} ion chromatography (IC),^{19,22,24–27} high pressure liquid chromatography (HPLC),¹⁷ electrospray ionization mass spectrometry (ESI-MS),^{17,22,24–27} infrared (IR) spectroscopy,²⁸ inductively coupled or low temperature plasma mass spectrometry (ICP-MS),^{22,26} (LTP-MS)²⁹ as well as optical emission spectroscopy (ICP-OES)^{22,25} or hyphenations of these methods was thoroughly reviewed.

Though most of these studies discuss qualitative data, the extent of HF release was estimated by titration with NaOH ⁸ while OPF_2OEt formation during electrolyte aging could be established

by nuclear magnetic resonance (NMR) spectroscopy.^{11,14} Other reports include a quantification of carbonates and their degradation products based on HPLC and GC methods,^{17,19} that in principle allow for a separation of non-ionic electrolyte components. Nevertheless, to the best of our knowledge, there is no detailed report available that quantitatively considers the degradation products of the rather abundantly applied electrolyte 1 M LiPF_6 in a mixture of ethylene carbonate (EC) and dimethyl carbonate (DMC) though unraveling of molecular electrolyte aging mechanisms could afford unprecedented ways to either prevent or at least defer occurring aging phenomena. Therefore, in this work, the impact of various experimental conditions on both the electrolyte stability and aging processes are systematically elucidated. In addition, monitoring the occurrence of potentially toxic compounds may yield crucial data for further industrial safety evaluations. Since the compounds likely involved in electrolyte aging contain NMR-active nuclei such as *e.g.*, fluorine, phosphorous or hydrogen multinuclear solution NMR spectroscopy is applied for identification and quantification of molecular species present in the considered aged electrolytes where the use of gas-tight flame-sealed NMR tubes with polytetrafluoroethylene (PTFE) tube liners should allow for equilibrium conditions at least at the timescale of the experiments.

2 Experimental

2.1 Materials

Battery grade SelectiLyte™ LP30 was purchased from BASF (Germany). It consists of LiPF_6 (1 mol L⁻¹) in EC:DMC (1:1 by weight). The water content of the electrolyte was

^a University of Muenster, MEET Battery Research Center, Institute of Physical Chemistry, Corrensstraße 46, 48149 Muenster, Germany.

E-mail: sascha.nowak@uni-muenster.de

^b Helmholtz Institute Münster, IEK-12 of Forschungszentrum Jülich, Corrensstraße 46, Münster, Germany

† Electronic supplementary information (ESI) available. See DOI: 10.1039/c6cp05276b



signal areas of EC and its associated decomposition products such as dimethyl-2,5-dioxahexane di-carboxylate (DMDOHC) and 2-methoxyethyl methyl carbonate (MEMC) in the corresponding ^1H or $^{13}\text{C}\{^1\text{H}\}$ solution NMR spectra ($I_0(\text{EC})$). The latter compounds are solely identified in the case of considerably aged electrolytes.

Based on quantitative ^1H or $^{13}\text{C}\{^1\text{H}\}$ and ^{19}F NMR data the actual PF_6^- concentration $c(\text{PF}_6^-)$ during electrolyte degradation can be obtained from the expression

$$c(\text{PF}_6^-) = c_0(\text{PF}_6^-) \cdot \frac{I(\text{PF}_6) \cdot I_0(\text{EC})}{I_0(\text{PF}_6^-) \cdot I(\text{EC})} \quad (1)$$

where c_0 is the initial concentration, I is the actual integrated signal area and I_0 the initial integrated signal area of the considered species. Note that this NMR based quantification approach requires steady acquisition parameters including NMR hardware aspects such as probe tuning and temperature control. Though in principle both the ^1H and $^{13}\text{C}\{^1\text{H}\}$ NMR signal of EC may be used as internal reference, the significantly narrower $^{13}\text{C}\{^1\text{H}\}$ signal is preferred. All quantitative data presented in this work is based on ^{19}F NMR signal areas of analytes and $^{13}\text{C}\{^1\text{H}\}$ NMR signal areas of heteronuclear standards. The suitability of NMR to reliably quantify the species of interest is documented by a dilution series of monofluorobenzene in acetonitrile with a constant concentration of DMC (Fig. 2). Indeed, the normalized integrated peak area ratios reflecting increasing contents of monofluorobenzene showed a good linearity and relative standard deviations (RSD) below 1% where the limit of quantification (LOQ) was found at $200 \mu\text{mol L}^{-1}$ corresponding to a fluorine content of 3.8 ppm. Subsequently, insight into the decomposition of PF_6^- in the presence of water was obtained from unambiguously monitoring the concentration of HF, OPF_2OH , OPF_2OMe and monofluorinated phosphates, respectively. The results are utilized to refine or augment previously reported PF_6^- degradation schemes (Fig. 3),^{11,16,25,26}

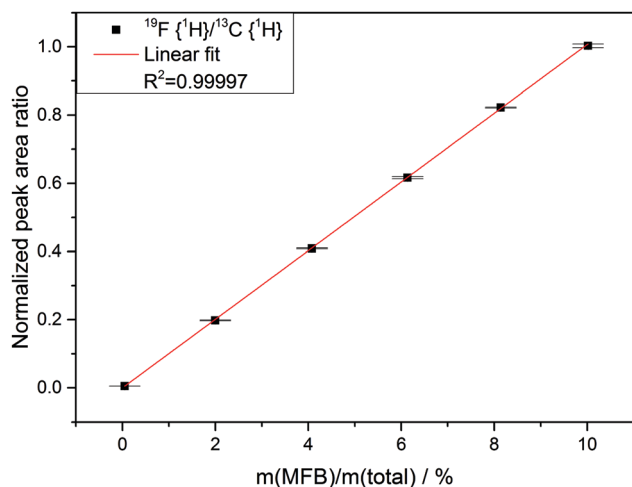


Fig. 2 Dilution series of monofluorobenzene (MFB) in acetonitrile with a constant concentration of DMC. Normalized peak area ratio obtained from $^{19}\text{F}\{^1\text{H}\}$ and $^{13}\text{C}\{^1\text{H}\}$ NMR measurements. The lowest of the plotted data points is 0.05% (wt) MFB.

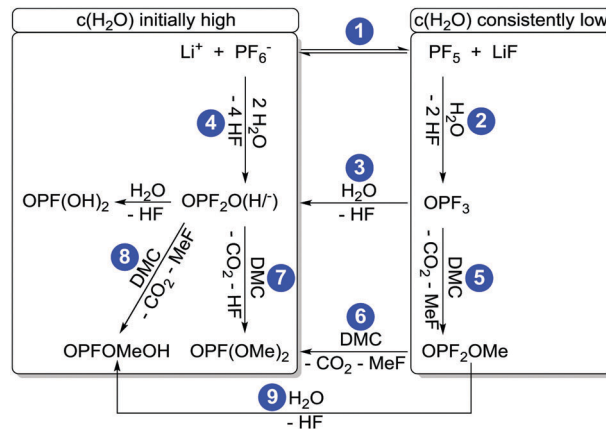


Fig. 3 Proposed reaction scheme of PF_6^- degradation. Frames highlight predominant “linear” reaction routes in the case of initially added high amounts of water (LP30 + H_2O , PTFE) and in the presence of rather low concentrations of water (LP30, glass).

while expanding molecular understanding of the underlying reaction steps.

Due to hydrolysis of PF_5 and PF_6^- (reaction routes 2 and 4) HF will be released at the onset of degradation, therefore the concentration curves of HF in case of three different types of samples were observed (Fig. 4) for a period of 56 days. As anticipated all the samples with an addition of 1000 ± 10 vppm of water exhibited a rather strong increase of the HF concentration to $110 \pm 5 \text{ mmol L}^{-1}$ after one day, which is twice the initial water concentration ($55.6 \pm 0.6 \text{ mmol L}^{-1}$) and in agreement with reaction route 4 (and possibly 1, 2 and 3). The subsequently identified decrease of the HF concentration suggests that HF in part even escaped from the PTFE NMR tube, though no significant impact on the actual mechanism of electrolyte degradation is expected. In contrast, the samples without water addition revealed much lower HF concentrations. For “LP30, PTFE” the HF concentration rather slowly

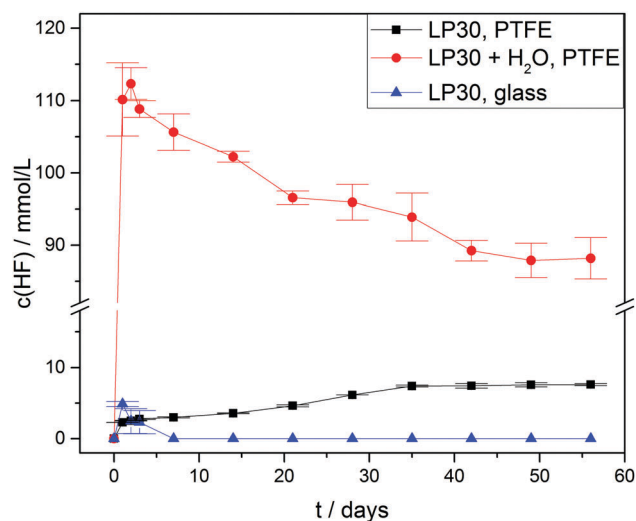


Fig. 4 HF concentration curves of LP30 stored at $60 \text{ }^\circ\text{C}$. Lines serve as guide to the eye.



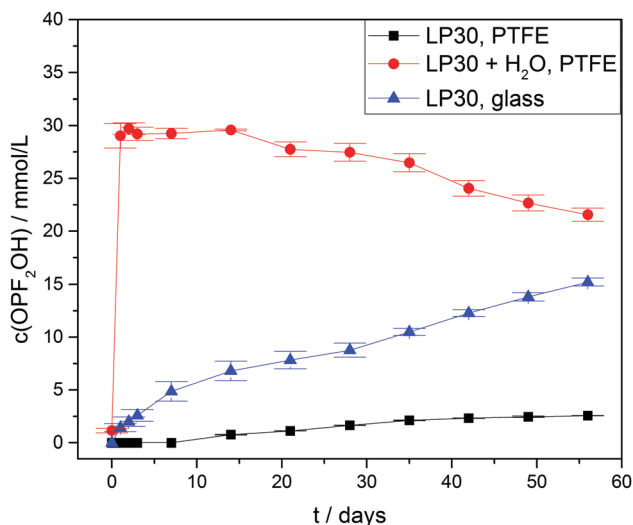


Fig. 5 OPF₂OH concentration curves of LP30 stored at 60 °C. Lines serve as guide to the eye.

increased to $7.6 \pm 0.2 \text{ mmol L}^{-1}$ after eight weeks while negligibly small amounts of HF were detectable in case of “LP30, glass” during the first days. In the latter sample, HF disappeared after one week due to the reaction with the NMR glass tube yielding BF_4^- and H_2O . Notably, the concentration of OPF₂OH rapidly increased in the samples with water addition, thus during one day reaching $29 \pm 1.2 \text{ mmol L}^{-1}$ (Fig. 5) in agreement with reaction route 4. The subsequent decrease of OPF₂OH concentration to $21.6 \pm 0.6 \text{ mmol L}^{-1}$ during the observation period of 56 days is attributed to substitution reactions according to reaction routes 7 and 8, yielding monofluorinated phosphates. Likewise, for the samples stored in glass tubes (LP30, glass) the concentration of OPF₂OH increased continuously to a value of $15.2 \pm 0.4 \text{ mmol L}^{-1}$ at the end of the measurement period, reflecting the reaction of

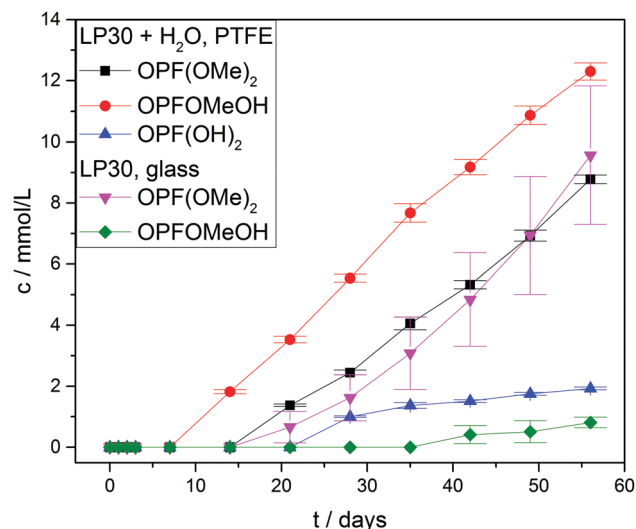


Fig. 7 Concentration curves of monofluorinated phosphates. Concentrations in the PTFE tube samples without water addition are below the LOQ. Lines serve as guide to the eye.

HF with glass and accompanied release of water that corroborate an ongoing formation of OPF₂OH. Without water addition the formation of OPF₂OH in the PTFE tube samples is almost negligible, reaching merely $2.56 \pm 0.01 \text{ mmol L}^{-1}$ after eight weeks.

For the difluorinated phosphates OPF₂OH and OPF₂OME remarkably different rates of formation were identified. While the formation of OPF₂OH was very pronounced in those samples where additional water was added ($21.6 \pm 0.6 \text{ mmol L}^{-1}$), the concentration of OPF₂OME solely reached $4.57 \pm 0.05 \text{ mmol L}^{-1}$ after eight weeks of aging (Fig. 6). In contrast, the samples stored in glass NMR tubes exhibited a maximum OPF₂OME concentration of $55.2 \pm 0.6 \text{ mmol L}^{-1}$ while for OPF₂OH a maximum concentration of $15.2 \pm 0.4 \text{ mmol L}^{-1}$ was determined. In principle, this observation may be rationalized based on the proposed reaction scheme (Fig. 3) provided that the reaction of PF₅ with water is favored over the reaction of PF₆⁻ with water. However, the presented equilibrium (reaction 1) is far on the left side (since the fresh electrolyte predominantly contains PF₆⁻) thereby promoting a reaction of water with PF₆⁻ so that it appears reasonable to assume that initially added water primarily reacts with PF₆⁻ until it is almost consumed (reaction path 4). In contrast, in the presence of rather small amounts of water the equilibrium reaction 1 could deliver sufficient amounts of PF₅ that further react with traces of water, in this way following the reaction paths 2 and 5. This scenario is feasible for the electrolytes stored in glass tubes where a minor amount of water is permanently present, hence suggesting that preferred reaction paths for electrolyte degradation are influenced by the overall amount of water present in the sample or eventually added and whether or not the critical amount of water is provided in one batch at first or continuously formed over time. It has to be noted that no NMR signals assigned to PF₅ are found, which is in agreement with its character as a highly reactive intermediate.

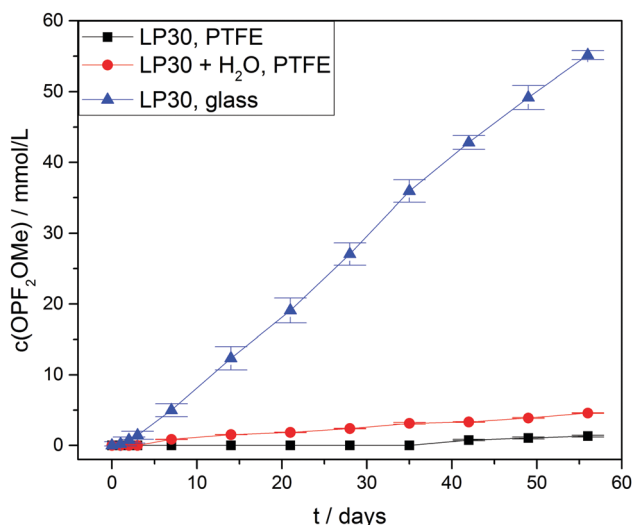


Fig. 6 OPF₂OMe concentration curves of LP30 stored at 60 °C. Lines serve as guide to the eye.



Fig. 7 shows the measured concentrations of monofluorinated phosphates. These degradation products were only found in the “LP30 + H₂O, PTFE” and “LP30, glass” samples. The concentrations in the samples with water addition show an almost constant slope, whereas the slope of OPF(OMe)₂ increases over time in the glass tubes. The reason for this is most likely the formation of the monofluorinated phosphates by a reaction of difluorinated phosphates with DMC (Fig. 3 reaction routes 6, 7 and 8). Reaction routes 6 and 8 are previously proposed based on qualitative data about electrolyte degradation products.^{22,26,29} The results of this work confirm these proposals. Furthermore, it has to be noted that only quantitative studies are able to reveal reaction route 7 by

comparing the product's formation rate with the reactants concentration. The formation of OPFOME₂ in the glass tube samples most likely proceeds according to reaction routes 8 and 9.

The autocatalytic reaction mechanism (Fig. 1) for the degradation of LiPF₆ in carbonate based solvents indicates the OPF₃ species as main driving force of the overall reaction where consumption of one OPF₃ molecule eventually results in the release of two further OPF₃ molecules, thereby accelerating the electrolyte degradation rate, accompanied by subsequent accumulation of OPF₃. The accumulation of OPF₃, however, was not observed within this work. Rather, the NMR based quantification of the occurring reaction species clearly

Table 1 Identified compounds found in thermally aged LP30 electrolyte, NMR signal specifications and concentrations *c* after eight weeks of aging at 60 °C

Compound	$\delta(^1\text{H})/\text{ppm}$ ($J(^1\text{H}-^1\text{H}), J(^1\text{H}-^{31}\text{P})$)	$\delta(^{13}\text{C}\{^1\text{H}\})/\text{ppm}$	$\delta(^{19}\text{F})/\text{ppm}$ ($J(^{19}\text{F}-^{31}\text{P})$)	$\delta(^{31}\text{P})/\text{ppm}$ ($J(^{19}\text{F}-^{31}\text{P}), J(^1\text{H}-^{31}\text{P})$)	<i>c</i> (<i>t</i> = 56 days)/ mmol ⁻¹ L ⁻¹ LP30; LP30 + H ₂ O; LP30 glass
EC	4.63 (s)	67.1 158.7	—	—	—
DMC	3.81 (s)	56.0 158.2	—	—	—
PF ₆ ⁻	—	—	-72.70 (d, 708 Hz)	-146.1 (sept, 708 Hz)	996 ± 16; 956 ± 20; 895 ± 8
CH ₃ OCH ₃	3.37 (s)	61.1	—	—	—
CH ₂ CH ₂	5.80 (s)	—	—	—	—
CO ₂	—	126.3	—	—	—
DMDOHC	4.41 (s)	67.2 157.3	—	—	—
MEMC	3.39 (s) 3.67 (t + d, 1.9, 9.1 Hz); 4.32 (t + d, 1.9, 9.1 Hz)	59.368.4 71.5 157.7	—	—	—
OPF ₃	—	—	-88.09 (d, 1066 Hz)	-36.3 (q, 1066 Hz)	<LOD; <LOD; 0.22 ± 0.01
OPF ₂ (OH)	—	—	-83.35 (d, 930–960 Hz)	-21.6 (t, 930–960 Hz)	2.56 ± 0.01; 21.6 ± 0.6; 15.2 ± 0.4
OPF ₂ (OMe)	4.22 (d, 12.0 Hz)	—	-86.59 (d, 1008 Hz)	-21.1 (t; q, 1008 Hz, 12.2 Hz)	1.3 ± 0.1; 4.57 ± 0.05; 55.2 ± 0.6
OPF ₂ (OCH ₂ CH ₂ OMe) ^a	4.51 (m) 4.77 (m)	—	-84.40 (d, 1007 Hz)	-21.9 (t; t, 1007 Hz, 9.4 Hz, 1.9 Hz)	<LOD; <LOD; 1.36 ± 0.02
OPF(OH) ₂	—	—	-75.76 (d, 926 Hz)	-10.6 (d, 926 Hz)	<LOD; 1.93 ± 0.05; <LOD
OPF(OMe)(OH)	3.98 (d, 11.7 Hz)	—	-82.18 (d, 943 Hz)	-10.2 (d; q, 943 Hz, 11.7 Hz)	<LOD; 12.3 ± 0.3; 0.8 ± 0.2
OPF(OMe) ₂	4.04 (d, 11.6 Hz)	—	-86.73 (d, 962 Hz)	-9.5 (d; sept, 962 Hz, 11.6 Hz)	<LOD; 8.8 ± 0.1; 10 ± 2
OPF ₂ (OH)-BF ₃	—	—	-84.40 (d; q, 960 Hz, 2.5 Hz) -147.78 (¹⁰ B) (d; t, 10 Hz, 2.5 Hz) -147.84 (¹¹ B) (d; t, 10 Hz, 2.5 Hz)	-27.6 (t; q, 960 Hz, 10 Hz)	<LOD; <LOD; 0.77 ± 0.05
BF ₄ ⁻	—	—	-154.22 (¹⁰ B), -154.27 (¹¹ B)	—	<LOD; 1.2 ± 0.1; 11.9 ± 0.2
HF	9.14 (d, 474 Hz)	—	-188.05 (d, 474 Hz)	—	7.6 ± 0.2; 88 ± 3; <LOD

^a The signal of the OMe-group was not found. LOD: limit of detection.



revealed that the degradation rates of pristine and aged electrolytes are comparable. In addition, the presence of OPF_3 (^{19}F NMR signal at -88.9 ppm) could be detected only in the case of samples stored in NMR glass tubes at rather constant amounts. These observations are not in favor of a “cyclic” autocatalytic reaction mechanism but corroborate electrolyte aging according to an augmented linear reaction scheme (Fig. 3).^{22,26,29}

Note that the reaction paths 6 and 8 were previously introduced based on qualitative inspection of electrolyte degradation products^{22,26,29} and are supported by this work while the reaction routes 4, 7 and 9 were identified from concentration curves and comparison of the concentrations of difluorinated phosphates with the formation rate of monofluorinated phosphates, hence from quantitative data of this work. Since the samples stored in PTFE tubes without the presence of water revealed minor degradation while all the others exhibited significant aging (as established from residual concentrations of PF_6^- after eight weeks, see Table 1) it appears that chemical instability of the electrolyte with respect to water rather than with respect to elevated temperatures is responsible for the observable degradation over time.

3.2 Identification

The identification of degradation products and assignment of their NMR signals are crucial steps prior to quantification. Besides the necessity of knowing the compounds that are to be quantified, it is required that all degradation products of the chosen heteronuclear standard (EC) are found. If EC is not completely stable, its degradation products have to be taken into account for an accurate quantification.

The ESI⁺ contain a detailed description of the identification strategy and the complex measurements which were necessary for the signal assignment. All identified compounds are listed in Table 1. Two compounds, namely dimethyl-2,5-dioxahexane dicarboxylate (DMDOHC) and 2-methoxyethyl methyl carbonate (MEMC) are found as degradation products of EC (Fig. S5, ESI⁺).

The ^{19}F NMR spectrum of electrolyte LP30 stored in NMR glass tubes at 60°C contains two singlets at approx. -154 ppm (Fig. 8). The ratio of their integrated signal areas is 1:4. According to literature the ^{19}F NMR signal of HF is a singlet at the same chemical shift.^{11,12,20} However, the ratio of the integrated signal areas is identical with the isotopic signature of boron (20% ^{10}B , 80% ^{11}B), suggesting the presence of BF_4^- formed by reaction of HF with the borate glass of the NMR tube. Furthermore, the ^{19}F NMR signal of BF_4^- is known to be at the above mentioned chemical shift.³¹ The different masses of the isotopes lead to different mean distances between the fluorine and boron atoms, which influences the chemical shift.³² The assignment to BF_4^- is confirmed by ^{19}F measurements of an electrolyte sample with additional LiBF_4 .

The actual HF signal in the ^{19}F NMR spectrum can be found when PTFE NMR tube liners are used. It is a doublet at -188.05 ppm with a $^1J(\text{H}-^{19}\text{F})$ coupling constant of 474 Hz

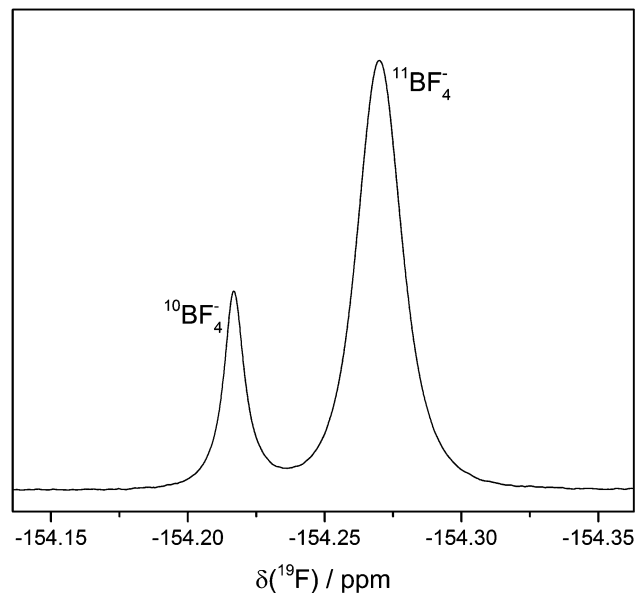


Fig. 8 ^{19}F signals of BF_4^- . LP30 stored in NMR glass tubes at 60°C . The two different singlets are caused by the two boron isotopes. Line broadening: 0.5 Hz.

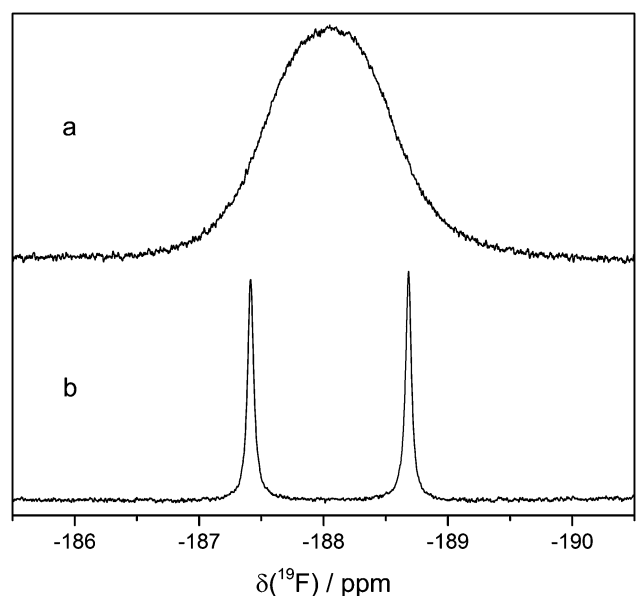


Fig. 9 ^{19}F signals of HF. Aged LP30 with (a) and without (b) water addition. Line broadening: 2 Hz.

(Fig. 9). To the best of our knowledge, this is the first time the $^1\text{H}-^{19}\text{F}$ coupling of HF is observed, most likely because the exchange of protons in the presence of protic compounds usually leads to the observation of a singlet. In this work, the addition of 1000 vppm water leads to broad singlets in the ^{19}F and ^1H spectra at the chemical shifts of HF. Fluoride and HF can form clusters of the formula $[\text{F}(\text{HF})_n]^-$.³³ Since the corresponding ^1H signal at 9.14 ppm is also a doublet, there is no more than one coupling partner of the ^1H hence no clusters are present.



5 Conclusions

A facile NMR method for reliable quantification of species occurring during thermal aging of electrolytes was developed and applied to expand the understanding of molecular processes thereby affording detailed insight into the underlying reaction mechanisms, which in principle are suitable for enhanced battery safety evaluations. In contrast to previous reports it was successfully demonstrated that electrolyte degradation proceeds at similar rates in pristine and already aged electrolytes upon thermal treatment. In addition, the collected NMR data strongly suggests that water not only reacts with PF₅ but also with PF₆⁻, in this way critically determining the actually occurring degradation products. While an excess of water forces hydrolysis of PF₆⁻ hence yielding OPF₂OH, the continuous presence of rather small amounts of water (*e.g.*, due to almost constant release from glass materials) results in predominant formation of OPF₂OME whereas negligible electrolyte degradation is observable in the absence of water, in this way highlighting the critical effects of different water concentrations in electrolytes.

Acknowledgements

The authors would like to thank the Bundesministerium für Bildung und Forschung (Federal Ministry of Education and Research, Germany) for funding the project “Elektrolytlabor 4e”.

References

- G. G. Amatucci, J. M. Tarascon and L. C. Klein, *J. Electrochem. Soc.*, 1996, **143**, 1114–1123.
- D. Aurbach, M. D. Levi, K. Gamulski, B. Markovsky, G. Salitra, E. Levi, U. Heider, L. Heider and R. Oesten, *J. Power Sources*, 1999, **81–82**, 472–479.
- A. K. Padhi, K. S. Nanjundaswamy and J. B. Goodenough, *J. Electrochem. Soc.*, 1997, **144**, 1188–1194.
- M. Winter, J. O. Besenhard, M. E. Spahr and P. Novák, *Adv. Mater.*, 1998, **10**, 725–763.
- T. Placke, V. Siozios, R. Schmitz, S. F. Lux, P. Bieker, C. Colle, H. W. Meyer, S. Passerini and M. Winter, *J. Power Sources*, 2012, **200**, 83–91.
- J. Kasnatscheew, M. Evertz, B. Streipert, R. Wagner, R. Klopsch, B. Vortmann, H. Hahn, S. Nowak, M. Amereller, A. C. Gentshev, P. Lamp and M. Winter, *Phys. Chem. Chem. Phys.*, 2016, **18**, 3956–3965.
- D. Aurbach, A. Zaban, A. Schechter, Y. Ein-Eli, E. Zinigrad and B. Markovsky, *J. Electrochem. Soc.*, 1995, **142**, 2873–2882.
- U. Heider, R. Oesten and M. Jungnitz, *J. Power Sources*, 1999, **81–82**, 119–122.
- S. E. Sloop, J. K. Pugh, S. Wang, J. B. Kerr and K. Kinoshita, *Electrochem. Solid-State Lett.*, 2001, **4**, A42–A44.
- B. Ravdel, K. M. Abraham, R. Gitzendanner, J. DiCarlo, B. Lucht and C. Campion, *J. Power Sources*, 2003, **119–121**, 805–810.
- C. L. Campion, W. Li and B. L. Lucht, *J. Electrochem. Soc.*, 2005, **152**, A2327–A2334.
- A. V. Plakhotnyk, L. Ernst and R. Schmutzler, *J. Fluorine Chem.*, 2005, **126**, 27–31.
- T. Kawamura, S. Okada and J.-i. Yamaki, *J. Power Sources*, 2006, **156**, 547–554.
- C. L. Campion, W. Li, W. B. Euler, B. L. Lucht, B. Ravdel, J. F. DiCarlo, R. Gitzendanner and K. M. Abraham, *Electrochem. Solid-State Lett.*, 2004, **7**, A194–A197.
- G. Gachot, S. Grugeon, M. Armand, S. Pilard, P. Guenot, J.-M. Tarascon and S. Laruelle, *J. Power Sources*, 2008, **178**, 409–421.
- W. Weber, V. Kraft, M. Grützke, R. Wagner, M. Winter and S. Nowak, *J. Chromatogr. A*, 2015, **1394**, 128–136.
- C. Schultz, V. Kraft, M. Pyschik, S. Weber, F. Schappacher, M. Winter and S. Nowak, *J. Electrochem. Soc.*, 2015, **162**, A629–A634.
- G. g. Gachot, P. Ribière, D. Mathiron, S. Grugeon, M. Armand, J.-B. Leriche, S. Pilard and S. p. Laruelle, *Anal. Chem.*, 2010, **83**, 478–485.
- M. Grützke, V. Kraft, W. Weber, C. Wendt, A. Friesen, S. Klamor, M. Winter and S. Nowak, *J. Supercrit. Fluids*, 2014, **94**, 216–222.
- P. Handel, G. Fauler, K. Kapper, M. Schmuck, C. Stangl, R. Fischer, F. Uhlig and S. Koller, *J. Power Sources*, 2014, **267**, 255–259.
- L. Terborg, S. Weber, S. Passerini, M. Winter, U. Karst and S. Nowak, *J. Power Sources*, 2014, **245**, 836–840.
- M. Grutzke, V. Kraft, B. Hoffmann, S. Klamor, J. Diekmann, A. Kwade, M. Winter and S. Nowak, *J. Power Sources*, 2015, **273**, 83–88.
- L. Gireaud, S. Grugeon, S. Pilard, P. Guenot, J.-M. Tarascon and S. Laruelle, *Anal. Chem.*, 2006, **78**, 3688–3698.
- L. Terborg, S. Nowak, S. Passerini, M. Winter, U. Karst, P. R. Haddad and P. N. Nesterenko, *Anal. Chim. Acta*, 2012, **714**, 121–126.
- L. Terborg, S. Weber, F. Blaske, S. Passerini, M. Winter, U. Karst and S. Nowak, *J. Power Sources*, 2013, **242**, 832–837.
- V. Kraft, M. Grützke, W. Weber, J. Menzel, S. Wiemers-Meyer, M. Winter and S. Nowak, *J. Chromatogr. A*, 2015, **1409**, 201–209.
- V. Kraft, M. Grutzke, W. Weber, M. Winter and S. Nowak, *J. Chromatogr. A*, 2014, **1354**, 92–100.
- S. Wilken, P. Johansson and P. Jacobsson, *Solid State Ionics*, 2012, **225**, 608–610.
- B. Vortmann, S. Nowak and C. Engelhard, *Anal. Chem.*, 2013, **85**, 3433–3438.
- S. K. Bharti and R. Roy, *TrAC, Trends Anal. Chem.*, 2012, **35**, 5–26.
- V. N. Plakhotnyk, L. Ernst, P. Sakhaii, N. F. Tovmash and R. Schmutzler, *J. Fluorine Chem.*, 1999, **98**, 133–135.
- H. S. Gutowsky, *J. Chem. Phys.*, 1959, **31**, 1683–1684.
- I. G. Shenderovich, S. N. Smirnov, G. S. Denisov, V. A. Gindin, N. S. Golubev, A. Dunger, R. Reibke, S. Kirpekar, O. L. Malkina and H.-H. Limbach, *Ber. Bunsen-Ges.*, 1998, **102**, 422–428.

